

MIT Open Access Articles

Near-infrared optical properties and proposed phase-change usefulness of transition metal disulfides

The MIT Faculty has made this article openly available. **Please share** how this access benefits you. Your story matters.

Citation: Singh, Akshay et al. "Near-infrared optical properties and proposed phase-change usefulness of transition metal disulfides." Applied Physics Letters 115, 16 (October 2019):161902 © 2019 Author(s)

As Published: <http://dx.doi.org/10.1063/1.5124224>

Publisher: AIP Publishing

Persistent URL: <https://hdl.handle.net/1721.1/123312>

Version: Final published version: final published article, as it appeared in a journal, conference proceedings, or other formally published context



Terms of use: Creative Commons Attribution 4.0 International license



Near-infrared optical properties and proposed phase-change usefulness of transition metal disulfides

Cite as: Appl. Phys. Lett. **115**, 161902 (2019); <https://doi.org/10.1063/1.5124224>

Submitted: 12 August 2019 . Accepted: 30 September 2019 . Published Online: 14 October 2019

Akshay Singh , Yifei Li, Balint Fodor, Laszlo Makai, Jian Zhou, Haowei Xu, Austin Akey, Ju Li, and R. Jaramillo 



View Online



Export Citation



CrossMark

ARTICLES YOU MAY BE INTERESTED IN

[Tuning of localized plasmon resonance in colloidal gold nano-particles by ultrafast interband photoinjection of free carriers: Superplasmonic states?](#)

Applied Physics Letters **115**, 161903 (2019); <https://doi.org/10.1063/1.5124950>

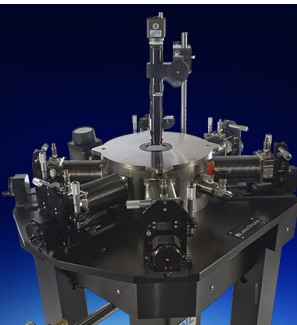
[Hybrid plasmonic metasurfaces](#)

Journal of Applied Physics **126**, 140901 (2019); <https://doi.org/10.1063/1.5116885>

[PFI-ZEKE-photoelectron spectroscopy of N₂O using narrow-band VUV laser radiation generated by four-wave mixing in Ar using a KBBF crystal](#)

The Journal of Chemical Physics **151**, 144302 (2019); <https://doi.org/10.1063/1.5124477>

 **Lake Shore**
CRYOTRONICS



Cryogenic probe stations

for accurate, repeatable
material measurements

LEARN MORE 

AIP
Publishing

Near-infrared optical properties and proposed phase-change usefulness of transition metal disulfides

Cite as: Appl. Phys. Lett. **115**, 161902 (2019); doi: [10.1063/1.5124224](https://doi.org/10.1063/1.5124224)

Submitted: 12 August 2019 · Accepted: 30 September 2019 ·

Published Online: 14 October 2019



View Online



Export Citation



CrossMark

Akshay Singh,¹  Yifei Li,¹ Balint Fodor,² Laszlo Makai,² Jian Zhou,³ Haowei Xu,⁴ Austin Akey,⁵ Ju Li,^{1,4} and R. Jaramillo^{1,a)} 

AFFILIATIONS

¹Department of Materials Science and Engineering, Massachusetts Institute of Technology, Cambridge, Massachusetts 02139, USA

²Semilab Semiconductor Physics Laboratory Co. Ltd., Budapest 1117, Hungary

³Center for Advancing Materials Performance from the Nanoscale, State Key Laboratory for Mechanical Behavior of Materials, Xi'an Jiaotong University, Xi'an 710049, China

⁴Department of Nuclear Science and Engineering, Massachusetts Institute of Technology, Cambridge, Massachusetts 02139, USA

⁵Center for Nanoscale Systems, Harvard University, Cambridge, Massachusetts 02138, USA

^{a)}rjaramil@mit.edu

ABSTRACT

The development of photonic integrated circuits would benefit from a wider selection of materials that can strongly control near-infrared (NIR) light. Transition metal dichalcogenides (TMDs) have been explored extensively for visible spectrum optoelectronics; the NIR properties of these layered materials have been less-studied. The measurement of optical constants is the foremost step to qualify TMDs for use in NIR photonics. Here, we measure the complex optical constants for select sulfide TMDs (bulk crystals of MoS₂, TiS₂, and ZrS₂) via spectroscopic ellipsometry in the visible-to-NIR range. We find that the presence of native oxide layers (measured by transmission electron microscopy) significantly modifies the observed optical constants and need to be modeled to extract actual optical constants. We support our measurements with density functional theory calculations and further predict large refractive index contrast between different phases. We further propose that TMDs could find use as photonic phase-change materials, by designing alloys that are thermodynamically adjacent to phase boundaries between competing crystal structures, to realize martensitic (i.e., displacive, order–order) switching.

© 2019 Author(s). All article content, except where otherwise noted, is licensed under a Creative Commons Attribution (CC BY) license (<http://creativecommons.org/licenses/by/4.0/>). <https://doi.org/10.1063/1.5124224>

Integrated photonics offers a way to create all-optical circuits to reduce the power needed to move and process massive data flows and to move beyond-von Neumann computing.^{1,2} Essential for photonic circuits are active materials that can modulate the phase and amplitude of light to perform switching, logic, and signal processing; if these changes are nonvolatile, then they can also be used for memory. The interaction length required to produce a substantial modulation of the optical phase is $L \sim \lambda_0/\Delta n$, where λ_0 is the free-space wavelength and Δn is the refractive index change. For instance, well established photonic material LiNbO₃ produces Δn of order 0.001 at typical supply voltages for electro-optic modulation and therefore requires a large interaction length $L > 1$ mm. A leading class of active materials that can strongly modulate near-infrared (NIR) light on a sub-micrometer length scale are the so-called phase-change chalcogenides, such as

those found in the Ge-Sb-Te (GST) system.³ These materials operate by switching between crystalline and amorphous phases, which produce refractive index changes $\Delta n > 1$, but suffer from high optical losses in the NIR and sub-gigahertz phase-change operation.^{4–6} There is a need to expand the selection of materials available for phase-change functionality in the NIR for integrated photonics.

Transition metal dichalcogenides (TMDs) are layered materials (van der Waals-bonded solids) with intriguing physical properties that include layer-number-dependent bandgap, electron pseudospin, exciton and trion excitations, chemical tunability, catalytic action, polymorphism and phase-change behavior, and strong above-bandgap light absorption.^{7–15} The NIR and below-bandgap optical properties of TMDs have been little-studied.^{16–19} TMDs interact strongly with light and are expected to feature low-loss for below-bandgap wavelengths.

Polymorphism suggests that transitions between structural phases, such as the trigonal prismatic 2H and octahedral 1T (or distorted 1T' and 1T_d), may be useful for optical switching.^{20,21} Transitions between 2H and 1T can be described by a simple translation of a plane of chalcogen atoms (a martensitic transformation).²² The layered, van der Waals crystal structure suggests that martensitic transformation strain may be low, which is beneficial for switching energy and fatigue. Phase-change functionality (i.e., transformation between layered polymorphs) at room-temperature has been demonstrated for tellurides including MoTe₂ and (Mo, W)Te₂.^{21,23–25}

In this manuscript, we focus on sulfide TMDs, because they have the largest bandgap (relative to selenides and tellurides) and therefore offer the largest spectral range for low-loss, below-bandgap operation. Unfortunately, the energetic cost of switching between phases is also highest for pure sulfides (relative to selenides and tellurides).^{23,26} We propose that alloying sulfide TMDs with different equilibrium structural phases, such as 2H MoS₂ and 1T TiS₂, could enable low-power switching. Specifically, these alloyed materials can be designed to be adjacent to a thermodynamic phase boundary.

Here, we measure the complex relative permittivity ($\epsilon = \epsilon_1 - i\epsilon_2$) of 2H-MoS₂, 1T-ZrS₂, and 1T-TiS₂ bulk crystals in the visible-to-NIR region (300–2100 nm), using spectroscopic ellipsometry (SE). We find that ϵ in the NIR cannot be simply extracted by extrapolating from visible-light measurements and requires explicit measurements. We find that spectroscopic measurements must account for the presence of native oxide to avoid overestimating NIR loss. We support our measurements with density functional theory (DFT) calculations, which further predict a large refractive index contrast between 2H and 1T phases. We then suggest a paradigm to use TMD alloys as active phase-change materials for integrated photonics and use DFT to calculate alloy phase stability.

Ellipsometry is a nondestructive optical technique that is widely used to measure the optical constants of thin films and bulk crystals.^{27,28} The technique involves measuring the ellipsometric ratio (ρ) of the amplitude reflection Fresnel coefficients for P- and S-polarized light (r_p and r_s , respectively) incident on a smooth surface. ρ is written as

$$\rho = \frac{r_p}{r_s} = \tan(\psi) \exp(i\Delta), \quad (1)$$

where ψ and Δ are the ellipsometric angles. ρ is a complex number and can be used to directly calculate real and imaginary optical constants, without relying on Kramers–Kronig (KK) relations. Relying on KK-constrained data can result in erroneous results, due to the extension of KK integral into spectral regions where measurements were not performed. Previous measurements have partially-characterized 2H-MoS₂ bulk crystals and thin films, with limited information in the NIR.^{29–33} Much less information is available for 1T-ZrS₂ and 1T-TiS₂.³⁴

We use thick TMD crystals to directly measure the dielectric properties in the NIR, without relying on models or extrapolation from visible-light measurements. For sufficiently-thick crystals, the light is absorbed completely, and there are no reflections from the back surface that can mix polarizations and cause measurement errors. We perform measurements on the mirrorlike faces of the as-received crystals, without any surface processing steps; below, we discuss how we account for the inevitable native oxide layer. We use two different

ellipsometry instruments (Semilab SE-2000, and J. A. Woollam UV-NIR Vase) to ensure repeatability (see the [supplementary material](#) for details).

The procedure for extracting ϵ from measurements of ρ is greatly simplified by using bulk crystal, as opposed to thin films. For a bulk, isotropic material, ϵ can be directly calculated as

$$\epsilon = \sin^2(\Phi) * \left(1 + \tan^2(\Phi) * \left(\frac{1 - \rho}{1 + \rho} \right)^2 \right), \quad (2)$$

where $\epsilon = \epsilon_1 - i\epsilon_2$, and Φ is the angle of incidence (AOI) relative to the surface normal direction.²⁷ ϵ calculated using Eq. (2) is called the “effective” permittivity and corresponds to a model of a pristine material interface with air, without a native oxide or any other overlayer. The presence of a native oxide can produce substantial errors including an overestimation of optical loss, as discussed below and in the [supplementary material](#).

We use the results of DFT electronic structure calculations to predict dielectric functions using the random phase approximation, as described in the previous work and in the [supplementary material](#).^{35,36} Briefly, we use Vienna *ab initio* simulation package (VASP), version 5.4.^{37–40} We treat the core and valence electrons by the projector-augmented plane wave method and approximate the exchange-correlation interaction by the generalized gradient approximation functional, implemented in the Perdew-Burke-Ernzerhof form.^{41,42} The energy minimization and force convergence criteria are 10^{-7} eV and 10^{-3} eV/Å, respectively.

The presence of a native oxide layer affects the experimental results in the entire spectral range and particularly for regions where the optical loss of the TMD is expected to be small, such as below the bandgap of MoS₂ and ZrS₂. We directly measured the thickness and composition of the native oxide using cross-sectional transmission electron microscopy (TEM) (see the [supplementary material](#)). On MoS₂, we find a rough surface, possibly including a native oxide, approximately 2 nm thick. On ZrS₂, we find a native oxide layer nearly 20 nm thick; similarly thick native oxide layers have been observed on ZrSe₂.⁴³ On TiS₂, we saw no native oxide, within the imaging resolution of our experiment (~ 1 nm). Adding these overlayers to the optical model used to analyze the ellipsometry data significantly affects the extracted permittivity of MoS₂ and ZrS₂ (see the [supplementary material](#) for modeling details).

In [Fig. 1](#), we present the experimentally-measured and theoretically-calculated in-plane complex permittivities for MoS₂, TiS₂, and ZrS₂. The experimental data in [Fig. 1](#) indicate the actual permittivity, determined by analyzing the ellipsometry data taking into account the native oxide layers. Of particular relevance for NIR photonics, ϵ_1 is large below the bandgap of MoS₂ and ZrS₂ (indirect $E_g = 1.1$ and 1.6 eV, respectively, indicated by solid gray lines); TiS₂ is a semimetal, (bandgap < 0.5 eV).^{18,34,44} The DFT calculations match fairly well the experimental data, both in magnitude and in spectral position of individual features. The A, B, and C excitons of MoS₂ are well-resolved.⁴⁵ For TiS₂, the experimentally-observed peaks match in energy but are substantially broader than those calculated by DFT and are qualitatively similar to previously-reported measurements of TiSe₂, indicating similar physical origins of the optical transitions.¹⁷ In ZrS₂, the strongest direct gap excitonic oscillators (2.5 and 2.9 eV) are observed in both experiment and theory, although the experimental

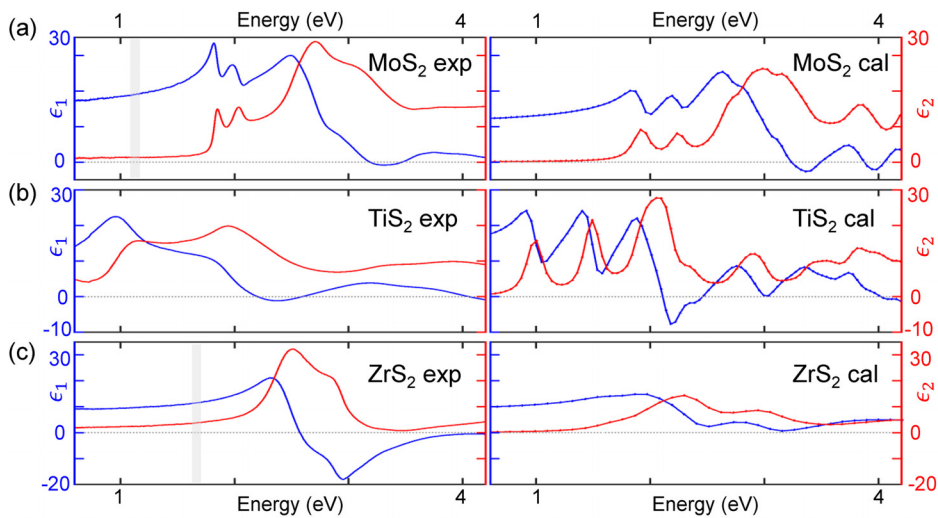


FIG. 1. NIR-VIS complex relative permittivity (ϵ) of sulfide TMDs. (Left column) Experimentally-measured permittivity at room-temperature and AOI = 70° by spectroscopic ellipsometry. (Right column) Calculated by DFT. Results shown for (a) 2H-MoS₂, (b) 1T-TiS₂, and (c) 1T-ZrS₂. The indirect bandgap of MoS₂ and ZrS₂ is indicated by light-gray lines.

data do not show the lowest-lying indirect gap transition near E_g . The 2.5 and 2.9 eV transitions are sufficiently close in energy to create zero-crossing of ϵ_1 near 3.2 eV, which is not seen in the DFT calculations. Further discussion of the various optical transitions can be found in the [supplementary material](#). Cross-polarization components are explicitly measured through generalized ellipsometry and are found to be ~ 0 for TiS₂ and MoS₂ (see the [supplementary material](#)).

The complex refractive index ($n - ik$) is related to ϵ by

$$n = \text{real}(\sqrt{\epsilon}), \quad k = -\text{imaginary}(\sqrt{\epsilon}). \quad (3)$$

k is related to the absorption coefficient ($\alpha = 4\pi k/\lambda$). In [Fig. 2](#), we plot experimentally-measured n and k in the NIR spectral region 0.6–1.5 eV (827–2067 nm). All three materials have large n , comparable to or larger than that of silicon ($n_{\text{NIR}} \approx 3.4$), which is appealing for guiding NIR light. MoS₂ and ZrS₂ are indirect-bandgap semiconductors and have low-loss in the NIR. TiS₂ is semimetallic and has higher loss.

The loss coefficients (k) determined by experiment and reported in [Fig. 2](#) are conditional on the particular samples measured and on our optical modeling and should be considered upper-bounds for these materials. In [Fig. 2](#), we indicate k determined from the effective permittivity [Eq. (3)], assuming no native oxide (dashed lines) and the value determined by optical modeling including native oxide thickness determined by TEM (solid lines). Taking the native oxide into account results in a lower value of the determined loss. Another important variable is the presence of defects, which contribute to below-bandgap absorption and optical loss. Our samples are bulk crystals (including a naturally-occurring specimen of MoS₂) and definitely contain defects, including sulfur vacancies that contribute to NIR absorption.⁴⁶ Measurements on synthetic MoS₂ monolayers have shown lower loss in the NIR.^{32,33} Our theoretical calculations are performed using models of perfect, defect-free crystals and predict substantially lower loss than the experiments (see [Fig. 1](#)). As the science of processing TMD materials improves, we will gain greater control over defects and can expect to have very low-loss TMDs for NIR applications.

We now address the question of the usefulness of phase change in sulfide TMDs as functionality for active materials. In [Fig. 3](#), we

show the calculated refractive index difference (Δn) between the 2H and 1T' phases of bulk MoS₂. We here show results for the 1T' phase instead of 1T because, according to our DFT calculations, 1T' has lower energy than 1T for monolayer MoS₂ and therefore 1T may spontaneously relax to 1T' in the zero-temperature limit. Compared to the 1T phase, the 1T' phase has lower in-plane symmetry due to Mo–Mo dimerization, leading to optical birefringence. In [Fig. 3](#), we have averaged the results for the principal in-plane axes for consistency with the experimental literature, in which there is little evidence for strong in-plane anisotropy at room-temperature (this could be due to ferroelastic domain microstructure, or a reduced order parameter at relatively high temperature). We find that Δn is large, comparable to or larger than that realized by phase-change materials in the GST system. The theoretically-predicted spectral features suggest photonics-relevant $\Delta n \sim 1$ throughout the NIR.

We focus on the NIR optical properties of sulfide TMDs because they offer lower optical loss (in NIR) than their selenide and telluride cousins, which have smaller bandgap. Unfortunately, the energetic cost of switching between phases is also highest for pure sulfides.^{23,25} Alloying sulfide TMDs with different reference states could enable low-power switching. The thermodynamics of TMD alloys are not well-established, and no phase diagrams have been published for the MoS₂-TiS₂-ZrS₂ ternary system, or the subsidiary binary systems. Here, we use DFT calculations to evaluate the likelihood of making binary alloys near the 2H-1T phase boundary (see the [supplementary material](#) for calculation details).

In [Fig. 4](#), we show the calculated Gibbs free energy-composition curves for the MoS₂-TiS₂ and MoS₂-ZrS₂ systems at 300 K. The results are very similar at 1000 K (not shown here), although with an overall downward shift of ~ 1 eV/f.u. (formula unit) relative to the data at 300 K. For both systems, the free energy curves for the 2H and 1T phases cross at an intermediate composition, which is suggestive of a phase boundary. For the MoS₂-TiS₂ system, the curves are concave-downward and lie above the convex hull, which for this system is a straight line connecting the pure phases. Therefore, MoS₂-TiS₂ alloys will have a tendency to phase-separate at equilibrium. For the MoS₂-ZrS₂, we predict a solid solution in the 2H structure for Mo_xZr_{1-x}S₂, $x > 0.75$, and phase

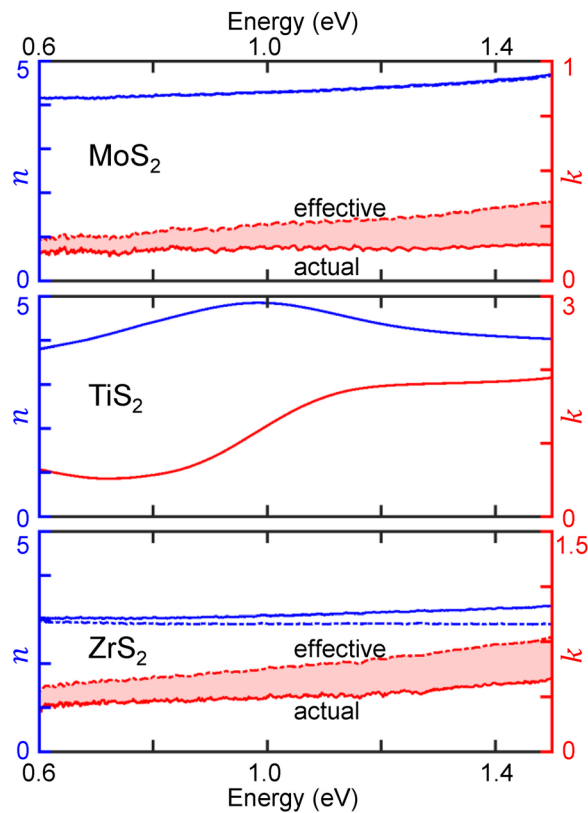


FIG. 2. Experimentally-measured real (n) and imaginary (k) refractive indexes of MoS_2 , TiS_2 , and ZrS_2 in the NIR spectral region. The solid lines (labeled “actual”) for MoS_2 and ZrS_2 are determined by modeling the ellipsometry data including native oxide layers. The dashed lines (labeled “effective”) represent the effective permittivity, which ignores the native oxide. The red shaded area represents experimental uncertainty (in k) due to potential misestimation of the native oxide thickness.

separation for more Zr-rich compositions. For both of these systems, the relatively small energy difference between the alloy curves and the convex hull (<1 eV/f.u.) suggests that alloys may be kinetically-stabilized near the 2H-1T phase boundary. The ZrS_2 - TiS_2 system is likely to be stable as a solid solution in the 1T phase, for which we do not calculate a

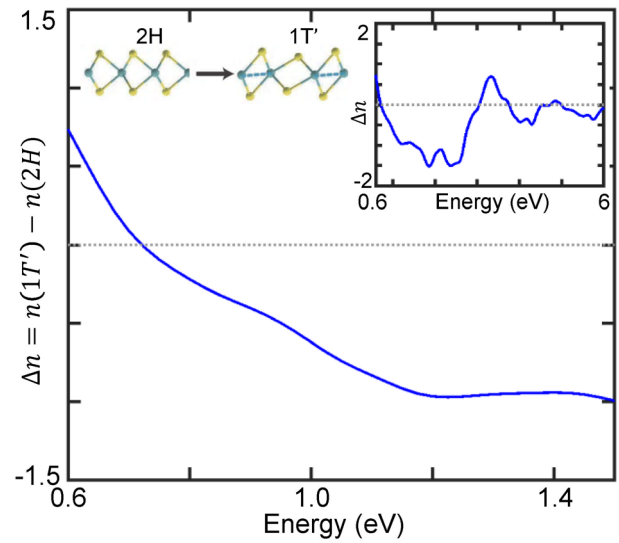


FIG. 3. Theoretically-predicted refractive index difference (Δn) between the 1T' and 2H phases of bulk MoS_2 in the NIR. (Inset, right) Δn over a wider energy range. (Inset, left) Illustrated change of atomic structure for 2H-1T' phase transition.

significant positive enthalpy of mixing and therefore do not expect to observe spinodal decomposition. Future work should consider metastability and the kinetics of phase separation in TMD alloy systems, and a particular focus on low-temperature processing of TMD alloy thin films.

We measure the complex optical constants of select sulfide TMDs in a spectral range from the visible to the NIR. The samples are single-crystals of 2H- MoS_2 , 1T- ZrS_2 , and 1T- TiS_2 and are chosen to represent prototypes of the 2H and 1T structure types. All materials have high index of refraction ($n \sim 3-4$), and MoS_2 and ZrS_2 feature low-loss in the NIR. We find that the presence of native oxides significantly changes the observed optical constants, and these oxide layers need to be characterized and modeled. Further, our DFT calculations predict a large refractive index and strong contrast in optical properties ($\Delta n \sim 1$) between the different structure (phase) types, suggesting a role for TMDs as phase-change materials for integrated photonics. Achieving this goal will require making materials that are thermodynamically-adjacent to a phase boundary. For sulfides, this will likely require

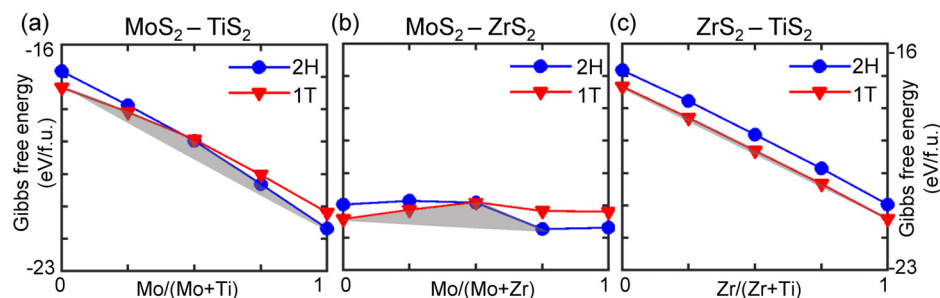


FIG. 4. Theoretically-predicted Gibbs free energy-composition plots for the (a) MoS_2 - TiS_2 , (b) MoS_2 - ZrS_2 , and (c) ZrS_2 - TiS_2 systems at 300 K. In the first two cases, the alloys are thermodynamically unstable relative to decomposition into pure phases. However, the free energy above the convex hull (gray zone) is small, which suggests that kinetic stabilization will be possible, e.g., through low-temperature processing. ZrS_2 - TiS_2 system is expected to form stable alloy solutions. We performed calculations for fully-relaxed structures. Therefore, the phase labeled “1T” in some cases has distortions akin to the 1T' phase.

alloying. We use DFT to calculate free energy-composition curves for alloys of MoS₂, ZrS₂, and TiS₂. The alloy structural phases become energetically degenerate at intermediate compositions, at which martensitic switching may be possible, if the alloys are found to be metastable or kinetically-stable.

See the [supplementary material](#) for information on: Experimental setup; attributing peaks to different transitions; transmission electron microscopy (TEM) characterization of surface; energy dispersive X-ray spectroscopy (EDS) of MoS₂ and ZrS₂ top surfaces; oxide and roughness modeling; TiS₂ with and without focusing optics; Mueller matrix (MM) measurements; theoretical calculations (DFT) for out-of-plane relative permittivity; multiple angle of incidence (MAI) measurements; effective ϵ for a range of ϵ_{\perp} and ϵ_{\parallel} , and for different angle of incidence (AOI); density function theory (DFT) calculations; phase diagram calculation; and comparison with previously published data for MoS₂.

This work was supported by an Office of Naval Research MURI through Grant No. N00014-17-1-2661. We acknowledge the use of facilities and instrumentation supported by NSF through the Massachusetts Institute of Technology Materials Research Science and Engineering Center DMR-1419807. This work was performed, in part, at the Center for Nanoscale Systems (CNS), a member of the National Nanotechnology Coordinated Infrastructure Network (NNCI), which is supported by the National Science Foundation under NSF Award No. 1541959. CNS is part of Harvard University. This work was performed, in part, at the Tufts Epitaxial Core Facility at Tufts University. We acknowledge assistance from the Department of Mineral Sciences, Smithsonian Institution. We acknowledge helpful discussions with Junho Choi, Yanwen Wu, Kevin Grossklous, John Byrnes, and Albert Davydov.

The authors declare no competing financial interest.

REFERENCES

- M. Asghari and A. V. Krishnamoorthy, *Nat. Photonics* **5**, 268 (2011).
- Y. Shen, N. C. Harris, S. Skirlo, M. Prabhu, T. Baehr-Jones, M. Hochberg, X. Sun, S. Zhao, H. Larochelle, D. Englund, and M. Soljačić, *Nat. Photonics* **11**, 441 (2017).
- M. Wuttig and N. Yamada, *Nat. Mater.* **6**, 824 (2007).
- N. Yamada, E. Ohno, K. Nishiuchi, N. Akahira, and M. Takao, *J. Appl. Phys.* **69**, 2849 (1991).
- H. S. P. Wong, S. Raoux, S. Kim, J. Liang, J. P. Reifenberg, B. Rajendran, M. Asheghi, and K. E. Goodson, *Proc. IEEE* **98**, 2201 (2010).
- B.-S. Lee, J. R. Abelson, S. G. Bishop, D.-H. Kang, B. Cheong, and K.-B. Kim, *J. Appl. Phys.* **97**, 093509 (2005).
- K. F. Mak, C. Lee, J. Hone, J. Shan, and T. F. Heinz, *Phys. Rev. Lett.* **105**, 136805 (2010).
- A. Splendiani, L. Sun, Y. Zhang, T. Li, J. Kim, C. Y. Chim, G. Galli, and F. Wang, *Nano Lett.* **10**, 1271 (2010).
- Y. Chen, J. Xi, D. O. Dumcenco, Z. Liu, K. Suenaga, D. Wang, Z. Shuai, Y.-S. Huang, and L. Xie, *ACS Nano* **7**, 4610 (2013).
- J. R. Schaibley, H. Yu, G. Clark, P. Rivera, J. S. Ross, K. L. Seyler, W. Yao, and X. Xu, *Nat. Rev. Mater.* **1**, 16055 (2016).
- A. Singh, K. Tran, M. Kolarczik, J. Seifert, Y. Wang, K. Hao, D. Pleskot, N. M. Gabor, S. Helmrich, N. Owschimikow, U. Woggon, and X. Li, *Phys. Rev. Lett.* **117**, 257402 (2016).
- A. Singh, G. Moody, S. Wu, Y. Wu, N. J. Ghimire, J. Yan, D. G. Mandrus, X. Xu, and X. Li, *Phys. Rev. Lett.* **112**, 216804 (2014).
- R. Lv, H. Terrones, A. L. Elías, N. Perea-López, H. R. Gutiérrez, E. Cruz-Silva, L. P. Rajukumar, M. S. Dresselhaus, and M. Terrones, *Nano Today* **10**, 559 (2015).
- K. F. Mak and J. Shan, *Nat. Photonics* **10**, 216 (2016).
- G. Fiori, F. Bonaccorso, G. Iannaccone, T. Palacios, D. Neumaier, A. Seabaugh, S. K. Banerjee, and L. Colombo, *Nat. Nanotechnol.* **9**, 768 (2014).
- N. Syrbu, V. Z. Cebotari, and N. P. Moldoveanu, *Jpn. J. Appl. Phys., Part 1* **35**, 6126 (1996).
- T. Buslaps, R. L. Johnson, and G. Jungk, *Thin Solid Films* **234**, 549 (1993).
- A. M. Goldberg, A. R. Beal, F. A. Lévy, and E. A. Davis, *Philos. Mag.* **32**, 367 (1975).
- G. Lucovsky, R. M. White, J. A. Benda, and J. F. Revelli, *Phys. Rev. B* **7**, 3859 (1973).
- L. Liu, J. Wu, L. Wu, M. Ye, X. Liu, Q. Wang, S. Hou, P. Lu, L. Sun, J. Zheng, L. Xing, L. Gu, X. Jiang, L. Xie, and L. Jiao, *Nat. Mater.* **17**, 1108 (2018).
- Y. Wang, J. Xiao, H. Zhu, Y. Li, Y. Alsaïd, K. Y. Fong, Y. Zhou, S. Wang, W. Shi, Y. Wang, A. Zettl, E. J. Reed, and X. Zhang, *Nature* **550**, 487 (2017).
- Y.-C. Lin, D. O. Dumcenco, Y.-S. Huang, and K. Suenaga, *Nat. Nanotechnol.* **9**, 391 (2014).
- K.-A. N. Duerloo, Y. Li, and E. J. Reed, *Nat. Commun.* **5**, 4214 (2014).
- W. Jin, T. Schiros, Y. Lin, J. Ma, R. Lou, Z. Dai, J.-X. Yu, D. Rhodes, J. T. Sadowski, X. Tong, T. Qian, M. Hashimoto, D. Lu, J. I. Dadap, S. Wang, E. J. G. Santos, J. Zang, K. Pohl, H. Ding, J. Hone, L. Balicas, A. N. Pasupathy, and R. M. Osgood, *Phys. Rev. B* **98**, 144114 (2018).
- F. Zhang, H. Zhang, S. Krylyuk, C. A. Milligan, Y. Zhu, D. Y. Zemlyanov, L. A. Bendersky, B. P. Burton, A. V. Davydov, and J. Appenzeller, *Nat. Mater.* **18**, 55 (2019).
- Y. Xiao, M. Zhou, J. Liu, J. Xu, and L. Fu, *Sci. China Mater.* **6**, 759 (2019).
- H. Fujiwara, *Spectroscopic Ellipsometry: Principles and Applications* (Wiley, 2007).
- D. den Engelsen, *J. Opt. Soc. Am.* **61**, 1460 (1971).
- A. R. Beal and H. P. Hughes, *J. Phys. C: Solid State Phys.* **12**, 881 (1979).
- J. W. Park, H. S. So, S. Kim, S.-H. Choi, H. Lee, J. Lee, C. Lee, and Y. Kim, *J. Appl. Phys.* **116**, 183509 (2014).
- D. Li, X. Song, J. Xu, Z. Wang, R. Zhang, P. Zhou, H. Zhang, R. Huang, S. Wang, Y. Zheng, D. W. Zhang, and L. Chen, *Appl. Surf. Sci.* **421**, 884 (2017).
- W. Li, A. G. Birdwell, M. Amani, R. A. Burke, X. Ling, Y.-H. Lee, X. Liang, L. Peng, C. A. Richter, J. Kong, D. J. Gundlach, and N. V. Nguyen, *Phys. Rev. B* **90**, 195434 (2014).
- H.-L. Liu, C.-C. Shen, S.-H. Su, C.-L. Hsu, M.-Y. Li, and L.-J. Li, *Appl. Phys. Lett.* **105**, 201905 (2014).
- S. C. Bayliss and W. Y. Liang, *J. Phys. C: Solid State Phys.* **15**, 1283 (1982).
- J. Zhou, H. Xu, Y. Li, R. Jaramillo, and J. Li, *Nano Lett.* **18**, 7794 (2018).
- M. Gajdoš, K. Hummer, G. Kresse, J. Furthmüller, and F. Bechstedt, *Phys. Rev. B* **73**, 045112 (2006).
- P. Hohenberg and W. Kohn, *Phys. Rev.* **136**, B864 (1964).
- W. Kohn and L. J. Sham, *Phys. Rev.* **140**, A1133 (1965).
- G. Kresse and J. Furthmüller, *Phys. Rev. B* **54**, 11169 (1996).
- G. Kresse and J. Furthmüller, *Comput. Mater. Sci.* **6**, 15 (1996).
- P. E. Blöchl, *Phys. Rev. B* **50**, 17953 (1994).
- J. P. Perdew, K. Burke, and M. Ernzerhof, *Phys. Rev. Lett.* **77**, 3865 (1996).
- M. J. Mleczko, C. Zhang, H. R. Lee, H.-H. Kuo, B. Magyari-Köpe, R. G. Moore, Z.-X. Shen, I. R. Fisher, Y. Nishi, and E. Pop, *Sci. Adv.* **3**, e1700481 (2017).
- D. L. Greenaway and R. Nitsche, *J. Phys. Chem. Solids* **26**, 1445 (1965).
- J. A. Wilson and A. D. Yoffe, *Adv. Phys.* **18**, 193 (1969).
- F. Fabbri, E. Rotunno, E. Cinquanta, D. Campi, E. Bonnini, D. Kaplan, L. Lazzarini, M. Bernasconi, C. Ferrari, M. Longo, G. Nicotra, A. Molle, V. Swaminathan, and G. Salviati, *Nat. Commun.* **7**, 13044 (2016).